Journal of Nepal Geological Society, 2022, Vol. 63, pp. 33–44
https://doi.org/10.3126/jngs.v63i01.50827

Landslide susceptibility assessment in the Rangun Khola watershed of far western Nepal

Lalit Pathak[1] and Krishna Chandra Devkota[2,*]

[1]Central Department of Environmental Science, Tribhuvan University, Kathmandu, Nepal
[2]Global Institute for Interdisciplinary Studies, Kathmandu, Nepal
**Corresponding author's email: kesandevkota@gmail.com*

ABSTRACT

Considering the serious threat of landslides to life, property, and the environment, this study aimed at exploring past landslides (2005-2020) to evaluate landslide susceptibility. The study is carried out in the Rangun Khola watershed, in western Nepal covering an area of 488 km^2. The landslide inventory map was prepared, recognizing 494 landslides, among them 70% were used for susceptibility mapping, and the rest 30% for validation purposes. The size of the landslide was found in the range of 103.53 m^2 to 149120.1 m^2, with an average of 4677.35 m^2. Frequency ratio (FR) and logistic regression (LR) models were implemented for landslide susceptibility assessment based on the various intrinsic factors. The validity of the models was assessed by using receiver operating characteristic (ROC) curves. The success rate was 87.6% for the LR model with a prediction rate of 87.3% indicating a good degree of fit. Similarly, with a success rate of 76.4% and a prediction rate of 75.1%, the result obtained from the FR model was a fairly good performance. Thus, both exhibited reasonably good accuracy in predicting the susceptibility of the landslide and are considered to be in land management and hazard mitigation, and policy formulating purposes.

Keywords: Frequency ratio, logistic regression, landslide susceptibility, Nepal Himalaya

Received: 22 March 2022 **Accepted:** 18 July 2022

INTRODUCTION

Nepal lies in the subduction zone between the Indian and Eurasian convergent plates making this area prone to various geo-hazards and associated disasters. Landslides are among the most frequent geo-hazards and major land degradation processes prevalent in the Himalaya (Dhakal, 2015). These landslides are the product of existing conditioning factors and complex interaction of various triggering factors (TU-CDES, 2016). Several natural conditioning factors as well as anthropic activities are prevalent within the Himalaya causing landslide incidents (Dhakal, 2014a). Unstable geological structures, soft and fragile rocks, common earthquakes, along with heavy and concentrated rainfalls during monsoon periods (Dahal and Hasegawa, 2008) are major natural factors leading to landslides and related phenomena in the rugged topography of Nepal (Dhakal, 2013; Dhital, 2000). Beside the inherent geology and natural characteristics; anthropic activities like poor linear infrastructure construction, improper land use, and mismanagement of the drainage leads to the evolution of landslide hazard (Dhakal, 2014a; Dhakal, 2014b). However the occurrence and risk of landslides varies with geological structure, rock and soil types, and geomorphology; rapid urban growth with increasing population and related phenomenon accelerating the landslide in Nepal (Petley et al., 2007).

The annual loss of lives and properties due to landslides is significantly high in the Himalayan region. It affects the lives and livelihoods of locals and the local economy along with psychological effects that can take decades to heal. During the summer monsoon, landslide has been mostly affecting infrastructure, lives, and properties in Nepal (Thapa, 2015). According to the data published by MoHA in Nepal Disaster Report (MoHA, 2019), a total of 483 landslide events were recorded causing 161 fatalities and affecting 1083 households with an estimated loss of $2 million during 2017/18. Apart from these many small-scale landslides go unreported; losing productive lands unless and until they involve the loss of life and properties or cause the blockage of the road (Dahal, 2012, Paudyal et al., 2021). The current study area, Rangun Khola watershed is regarded as prone to landslides and erosion events historically and now facing the development of urban features and other linear infrastructures (Dhakal, 2014b; Bhandari et al., 2021). Presence of active fault and erosional effect of seasonal rivers poses potentiality for landslide (Dhital, 2015) and related direct and indirect livelihood impacts in the area (Pathak et al., 2020; Bhandari et al., 2021). Although most of the incidents are not reported at national level but has significant ecological and economic. To minimize such losses, potential landslide-prone areas should, therefore, be recognized i.e. early detection of landslides probability (Schweigl and Hervas, 2009). In this respect, landslide susceptibility mapping can provide valuable information crucial for hazard mitigation through effective project planning and execution.

Susceptibility is the probability of an area to occur landslides. In mathematical form, landslide susceptibility can be considered as the probability of spatial occurrence of known slope failures, at a given set of geo-environmental situations (Guzzetti et al., 2005), which is considered as prerequisite for disaster management and planning development activities (Devkota et al., 2012). Susceptibility assessments can thus be used to predict the spatial distribution of future landslides based on the principle of uniformitarianism, which assumes that landslides

would occur in the future due to the same conditions that caused them in the past (Guzzetti et al., 2005). The first step toward susceptibility assessment is the identification and preparation of the Landslide Inventory Map (LIM) (Brabb, 1985; Galli et al., 2008). Based on inventory and conditioning factors susceptibility can be assessed applying various modeling approaches and GIS techniques (Pourghasemi et al., 2018).

Statistical approaches have been mostly used in landslide susceptibility assessment as it minimizes the subjectivity in the weightage assignment procedure (Pardeshi et al., 2013; Pourghasemi et al., 2018; Shao et al., 2020). Among the different statistical methods to prepare landslide susceptibility, most common models suggested in the literature are bivariate (Saha et al., 2005; Lee and Pradhan, 2007; Pradhan and Lee, 2010; Pardeshi et al., 2013; Pourghasemi et al., 2018; Shao et al., 2020) and multivariate (Lee and Talib, 2005; Pradhan and Lee, 2010; Devkota et al., 2012) and statistical techniques such as the logistic regression (Pourghasemi et al., 2018). Bivariate statistical analyses include the idea of comparing a landslide inventory map with maps of landslide conditioning factors to rank the corresponding classes according to their role in landslide formation. The ranking is generally carried out using the density of landslides. Multivariate statistical approaches uses two or more conditioning factors and evaluates which, if any, are correlated with a particular result. Other different methods have been proposed by several investigators, including weights-of-evidence methods (Pradhan et al., 2010; Regmi et al. 2014), certainty factors (Devkota et al., 2012), artificial neural networks (Lee, 2007), neuro-fuzzy (Sezer et al., 2011) etc. to evaluate the landslide susceptibility, with improved accuracy.

There are multiple studies in Nepal Himalaya focused on landslide susceptibility mapping using various approaches (Dhital et al., 1991; Pantha et al., 2008; Devkota et al., 2012; Regmi et al., 2014; Paudyal et al.,2021). These studies focus on to access physical properties of the landslides, geological settings, and associated loss of life and property, and study of the relationship between landslide occurrences and landslide conditioning factor needed to be studied for susceptibility mapping. The purpose of current study is to produce landslide susceptibility map of Rangun Khola watershed of Far-west Nepal using a bivariate statistical model i.e. Frequency Ratio (FR) and a multivariate statistical model i.e. logistic regression (LR). These models use data from the inventory map to predict where landslides might occur in the future and the results have been validated and reviewed.

MATERIALS AND METHODS

Study area

Rangun Khola is one of the seven watersheds within the Mahakali River Basin of Nepal having an area of 489.39 sq. km (Fig. 1). The watershed ranges from a tropical climate in the south to a temperate in the north with an elevation range from 2,500 m in the north, near the Mahabharat range, to 258 m in the southern part where the watershed flows into the Mahakali River at Parshuramdham (Pathak and Devkota, 2022). The population of the Rangun Khola watershed is 53,109 (CBS, 2011), and includes parts of the Doti and Dadeldhura districts in Sudurpaschim Province of Nepal. The average annual temperature ranges between 10°C to 25°C, and the annual average rainfall in the watershed is 1,346.6 mm, with the highest amount falling in the month of July (448.4 mm) and the lowest in November (7.3 mm) (Bhandari et al., 2021).

Based upon the digitization of map (Physiographic divisions of Nepal) (Dhital, 2015), the topography is characterized by a complex mixture of Siwalik 29% (lower, middle, and upper), Dun valley 20 %, and the 51% of Mahabharat range. The geology of the watershed is characterized by Boulder, cobble, grey mud and conglomerates in upper Siwalik region. Lower Shiwalik consists of fine-grained sandstones shales and siltstones whereas precambrian high grade metamorphic rocks comprising gneisses, quartzites and marbles are frequent over upper part. An active fault passes close to the main boundary thrust and runs through Budar, Alital, and Kalena depicted in (Fig. 1) (Dhital, 2015). This existing geology and topography make this area prone to landslide hazards. Several historical and present landslides are prevalent in this area (Pathak and Devkota, 2022). Thus, the study of landslides and their causative factors for determining susceptibility is necessary for this area.

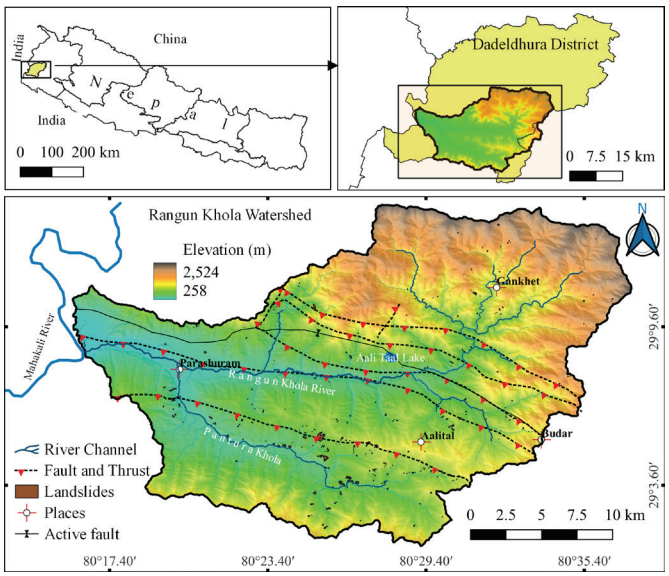

Fig. 1: Location map of the study area.

Methodology

In this study, bivariate and multivariate techniques for the Landslide Susceptibility mapping were applied. Preparation of the LSM in this study involved data collection, inventory map preparation, selection and preparation of Landslide Conditioning Factors (LCFs), LSM preparation using Frequency Ratio (FR), and Logistic Regression (LR) models and validation of the models (Fig. 2). Both primary and secondary data were used. The LIM was prepared based on the field investigation, satellite images, and Google Earth imagery. The topographic parameters of elevation, slope gradient, aspect, slope curvature, stream power index (SPI), drainage density, and topographical wetness index (TWI) were obtained from the 12.5×12.5 m resolution ALOSPALSAR DEM obtained from the Alaska Satellite Facility homepage. The geological map was acquired from the Department of Mines and Geology (DMG, 2020). NDVI and LULC were

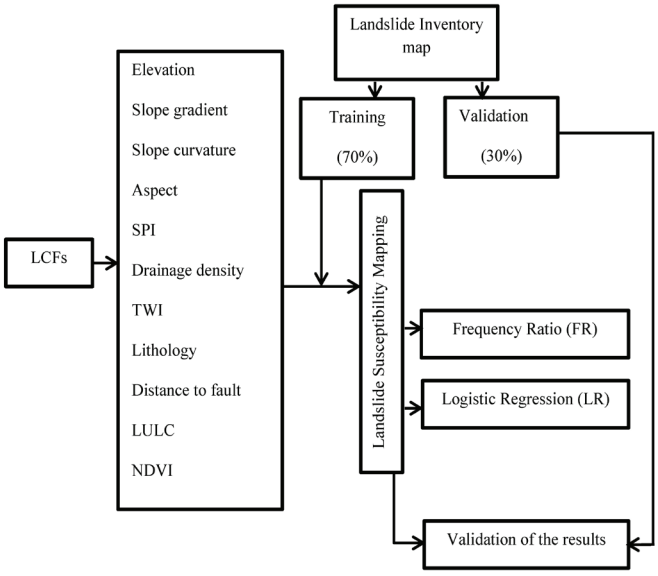

Fig. 2: Methodological flowchart of the study.

prepared by using Sentinel 2 images. The LSM is classified into five classes using the natural break method of Jenks. The whole process was carried out using R studio and QGIS.

Landslide inventory map (LIM)

Landslide Inventory Mapping (LIM) is an essential part of landslide susceptibility mapping. The relationship between the landslide inventory datasets and LCFs is the most important for landslide susceptibility mapping (Yilmaz et al., 2011). LIM can be prepared based on a combination of several data sources, including previous records, local field examinations, and the perception survey with inhabitants and interpretation of satellite images. Many landslides, due to their remote locations, undetectable in field surveys, can be extracted with acceptable resolution using Google Earth's optical images. For this study polygon-based spatiotemporal LIM was prepared from 2005 to 2020 based on both the desk study (satellite images, Google Earth imagery, and different published and unpublished reports) and field visit (GPS and landslide inventory form).

Landslide conditioning factors (LCFs)

Field surveys and review of previous literatures (Dhital et al., 1991; Pantha et al., 2008; Devkota et al., 2012; Regmi et al., 2014; PCTMCDB and TU-CDES, 2017) were carried out to select the landslide conditioning factors for this study. Eleven LCFs were considered with significant contribution were elevation (Fig. 3A), slope (Fig. 3B), plan curvature (Fig. 3C), slope aspect (Fig. 3D), topographic wetness index (Fig. 3E), stream power index (SPI) (Fig. 3F), drainag density (Fig. 3G), lithology (Fig. 3H), distance from fault (Fig. 3I), normalized difference vegetation index (NDVI) (Fig. 3J), and land use land cover (LULC) (Fig. 3K). The topographic factors elevation, slope gradient, aspect, slope curvature, stream power index (SPI), drainage density, and topographical wetness index (TWI) were obtained from the 12.5×12.5 m resolution ALOSPALSAR DEM which was acquired from Alaska Satellite Facility homepage. Lithology and distance form fault were acquired from Geological Map of Sudurpaschim acquired form DMG (2020). NDVI was calculated using red band and NIR band (NDVI = (NIR-RED)/(NIR+RED)) of Sentinel 2 images. Similarly land use and cover map was prepared with maximum likelihood classification of Sentinel 2 images. Table 1 depicts the range of parameters used for classification, along with their classes and methods.

Elevation is frequently used LCF for landslide susceptibility studies. It is stated that the landslides have more tendency to occur at higher elevations (Ercanoglu et al., 2004). The slope aspect or the direction of maximum slope of the terrain surface is divided into nine classes this can influence landslide in the way the direction of wind sunlight and also the amount of rainfall get influenced by aspect. The slope gradient is one of the most important factors that influence slope stability (Bednarik et al., 2010). The slope curvature represents the morphology of the topography (Devkota et al., 2012). The curvature maps were obtained from the second derivative of the surface and the absorption percolation and speed of water flow get influenced by this. Drainage density is also one of the landslide conditioning factors, which is a measurement of the sum of the channel lengths per unit area. SPI measures the erosion power of the stream and is also considered as a factor contributing toward stability within the study area and TWI combines local upslope contributing area and the entire slope, is commonly used to quantify topographic control on hydrological processes. Faults are the tectonic breaks that usually decrease the rock strength and play vital role in instabilities. Lithology is also an important in determining the susceptibility due different susceptibilities of geological units to existing geomorphic phenomenon (Pradhan and Lee, 2010). Similarly, LULC and NDVI also plays major role in slope stability and greatly influence landslide occurrence.

Landslide susceptibility modeling

Frequency ratio (FR) model

Frequency ratio is a successfully observation-based bivariate statistical approach for landslide susceptibility assessment (Pham et al., 2015). This model is based on the assessment of the observed spatial relationship between past landslides and a set of landslides contributing factors. It is carried by summation of the frequency ratio values that are the ratio of the probability of present and absence of landslide occurrences for each landslide conditioning factor class (Eq. 1) (Lee and Pradhan, 2007).

$$FR_i = \frac{P_i}{PL_j} \quad (1)$$

where, P_i is the percentage of pixels in each landslide conditioning factor class, PL_i is the percentage of landslide pixels in each landslide conditioning factor class and FRi is the frequency ratio of each conditioning factor (Eq. 2).

$$LSA = \sum FR_i \quad (2)$$

where, LSA is landslide susceptibility index and FR_i is the FR of each factor range.

Generally, FR value 1 is an average value; a value higher than 1 means higher correlation, and a value lower than 1 means lower correlation.

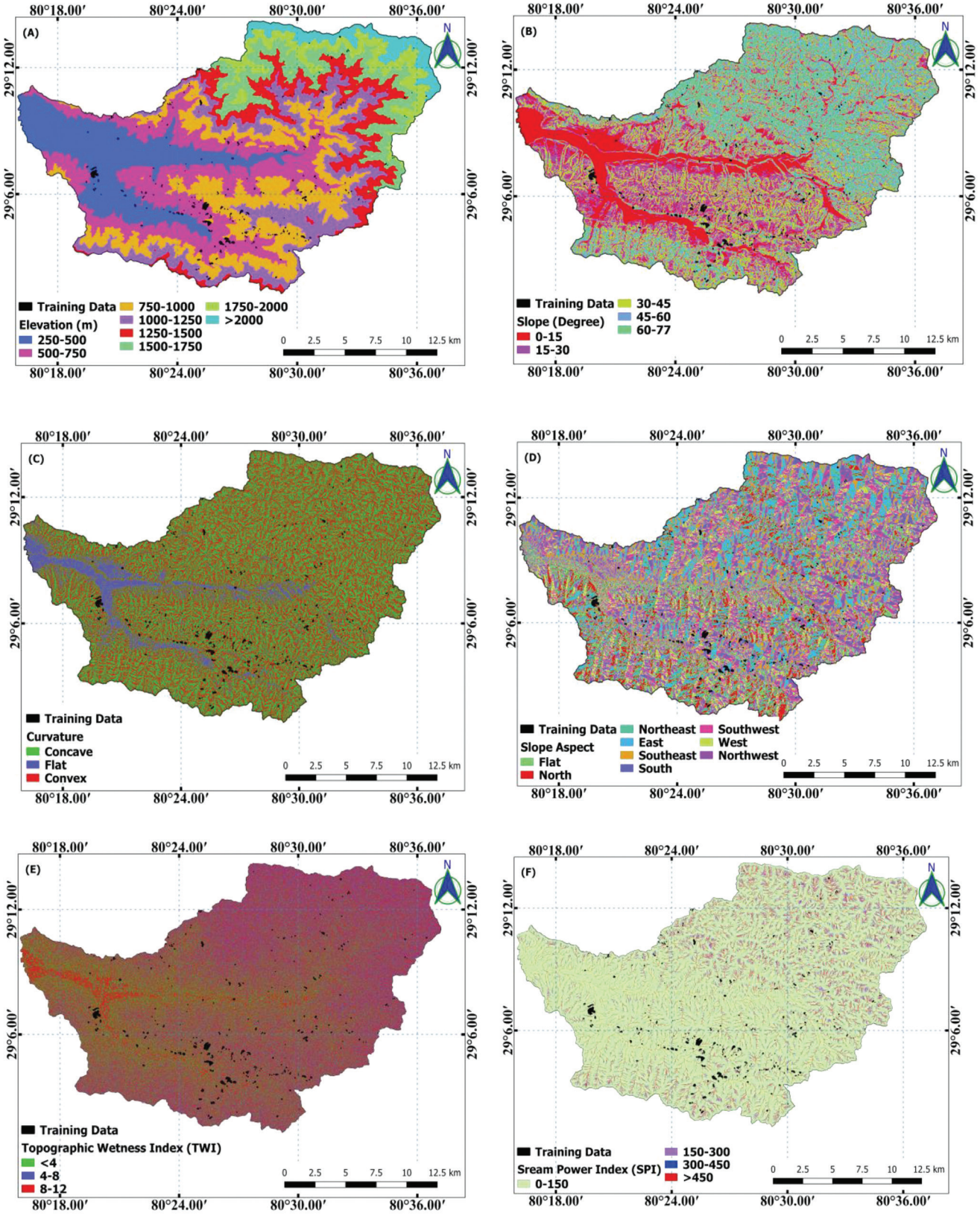

Fig. 3: Landslide conditioning factors: (A) Elevation, (B) Slope angle, (C) Plan curvature, (D) Slope aspect, (E) Topographic wetness index (TWI), (F) Stream power index. *Continued...*

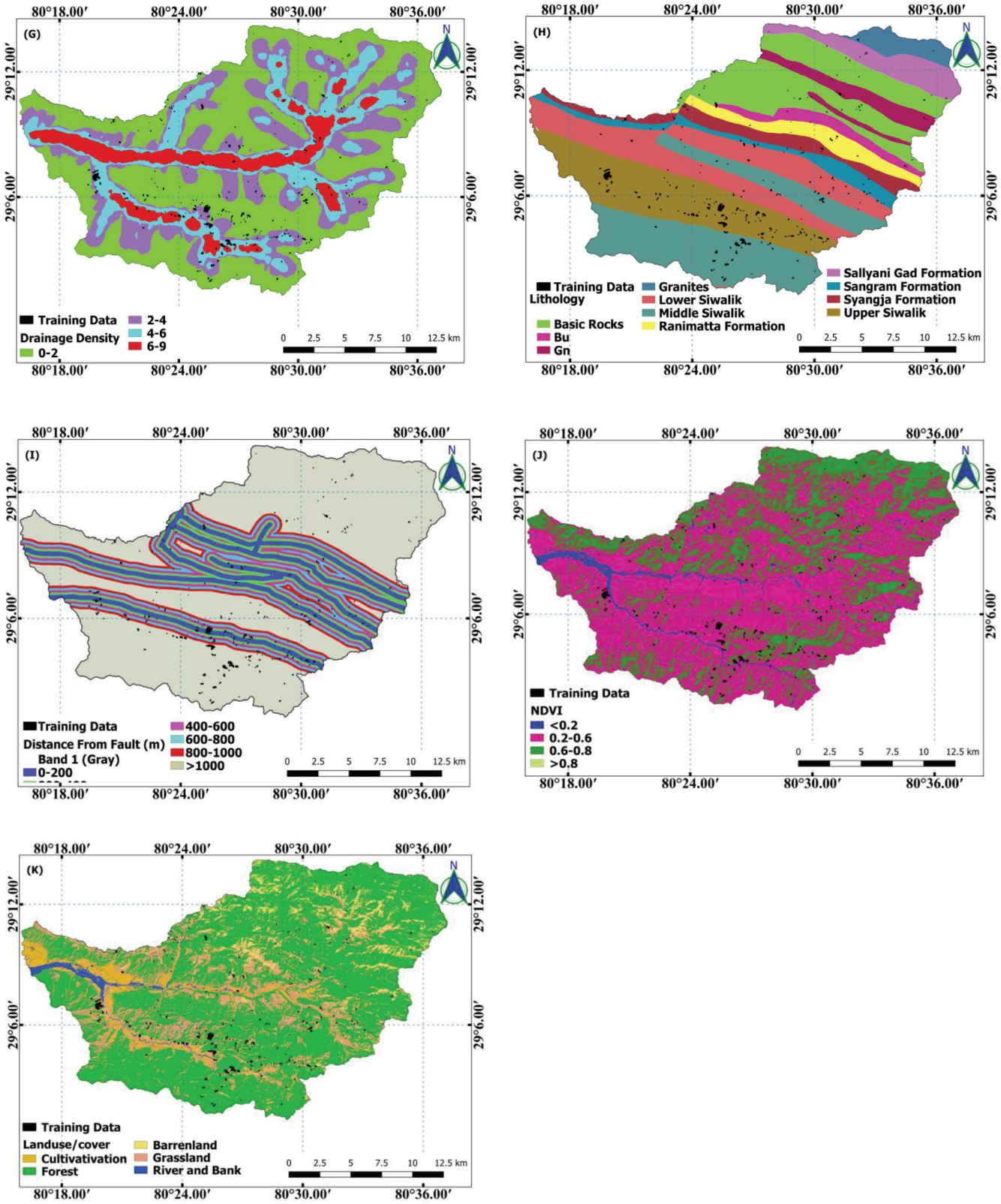

Fig. 3: Landslide conditioning factors: (G) Drainage density, (H) Lithology, (I) Distance to fault, (J) NDVI, (K) Land use/land cover (LULC).

Table 1: Data used for the preparation of LCFs analysis technique and classification.

LCFs	Data Used/Resolution	Technique	References
Elevation (m)	ALOSPALSAR DEM(12.5×12.5 m)	By using the DEM the elevation range (250-2500 m) was classified into eight classes.	(Li et al., 2004)
Slope Gradient (°)	ALOSPALSAR DEM(12.5×12.5 m)	$\text{Tan}\ \theta = \frac{N*i}{636.6}$ where, N = No. of Contour Cuttings	(Pradhan and Lee, 2010)
Plane Curvature	ALOSPALSAR DEM(12.5×12.5 m)	Using the DEM, plane curvature was classified into concave-convex and plane.	(Li et al., 2004)
Slope Aspect	ALOSPALSAR DEM(12.5×12.5 m)	Using the DEM slope aspect was determined.	
SPI	ALOSPALSAR DEM(12.5×12.5 m)	$SPI = \text{As}\tan\beta$ where A_s = the specific catchment area and β = local slope gradient.	(Moore and Grayson, 1991)
Drainage Density	ALOSPALSAR DEM(12.5×12.5 m) (l/km^2)	$\text{Drainage density} = \frac{\text{stream-length summation}}{Total\ area}$	
TWI	ALOSPALSAR DEM(12.5×12.5 m resolution)	$\text{TWI} = \ln\left(\frac{a}{\tan\beta}\right)$ Where, a= cumulative upslope area draining through a point (per unit contour length) and tanβ = e slope.	(Moore and Grayson, 1991)
Lithology	DMG (2020), Dhital (2015) and Shrestha et al.(1985)	Digitization process	(Dhital, 2015)
Distance to fault	Geological data from Dhital (2015) and DMG (2020)	Digitization and then Euclidian Distance Buffering	
LULC	Sentinel 2 (9.5×9.5 m)	Supervised classification (Maximum likelihood)	
NDVI	Sentinel 2 (9.5×9.5 m)	NDVI = (NIR-R) / (NIR+R), Where NIR is near inferred band R is the red band (NIR=B8, Red=B4)	(D'Odorico et al., 2013)

Logistic regression (LR) model

Logistic regression is the most commonly used multivariate statistical approach used in predicting the presence or absence of characteristics based on values of a set of predictor variables (Budimir et al., 2015). Considering p independent variables, x1, x2, ... , xp, affecting landslide occurrences, we define the vector X = (x1, x2, ... , xp). In this study, the independent variables were considered with values of 1 (presence) or 0 (absence).

In its most simple form the logistic regression model can be quantitatively expressed as (Eq. 3):

$$P=1 / (1+e^{-z}) \quad (3)$$

where, p is the probability of an event occurring, e is the constant 2.718 and, and z is the linear combination (Eq. 4):

$$Z= b0+ b1x1 + b2x2+ b3x3+bnxn \quad (4)$$

where, b0 is the intercept of the model, bi (i= 0,1, 2, 3 …. n), are the slope coefficient of the logistic regression model and, xi (i= 0, 1, 2, 3, n), are the independent variables the linear model is formed.

The logistic regression analysis was performed in R studio with exported data from GIS software to obtain the coefficients of the landslide conditioning factors.

Validation of the models

Validation was performed by using the area under the curve (AUC) of the receiver operating characteristic (ROC) curve. The AUC value ranges from 0.5 to 1 with AUC value 1 indicating perfect prediction. The ROC curve was plotted 1-specificity on the x-axis versus and sensitivity on the y-axis. The sensitivity and specificity were computed using the following equations 5 and 6.

$$Sensitivity = \frac{TP}{TP + FN} \quad (5)$$

$$Specificity = \frac{TN}{TN + FP} \quad (6)$$

where, TP (true positive), TN (true negative), FP (false positive), and FN (false negative).

The success rate curve was generated using the training dataset (70% landslides) while the prediction rate is developed using the validation dataset (30%). The success rate represents how well the resulting landslide map is classified using the existing landslides while the prediction rate indicates the predictive power of the landslide susceptibility model (Budimir et al., 2015).

RESULTS

Landslide inventory

In total, 494 landslides were identified in the study area including recent and old events based on both the desk study (satellite images, Google Earth imagery, and different published and unpublished reports) and field observation. The size of the individual landslide was found in the range of 103.53m^2-149120.1 m^2, with an average size of 4677.35 m^2, which ultimately covers the area of 2301058.62 m^2. The total area covered by the landslide is about 0.47% of the study. Landslides size greater than 100 m^2 were considered in the study as very small sizes were very difficult to identify remotely and precisely. Of the 494 landslides 70% (346 landslides) were randomly used for training the susceptibility models and the rest 30% (148/494) were used for validation of the models.

Landslide susceptibility

Landslide susceptibility map using frequency ratio (FR) model

The susceptibility of the landslide was determined based on the frequency ratios of the all eleven LCFs considered in this study. The numbers of the pixel in each class of LCFs were counted and ratio of the frequency was determined for each class, and a relationship was established between those factor and landslide occurrence. The final susceptibility map developed from this model is shown in Figure 4.

The susceptibility range of the landslide obtained by FR model was categorized into five classes namely Very low, Low, Moderate, High and Very high based upon natural break technique. In the study area largest portion falls under the high susceptibility zone which covers 27.98% of the total area. Similarly 19.74%, 18.29%, 18.68%, and 15.31% area is covered by moderate, low, very low and very high susceptibility zone, respectively (Fig. 5).

Investigating the effect of each class of on landslide occurrence using the FR method (Table 2) showed that landslide densities are higher in elevation range between 500-750 m followed by 750-1000 m. A slope gradient greater than 60 degrees is highly susceptible whereas less than 15 degrees is the lowest. Concave curvature is in the highly susceptible zone with a higher number of pixels than convex plane curvature. The FR from the slope aspect analysis shows that the S and SE-facing slopes are most affected by landslides, followed by NE, and E-facing slopes (Table 2). Similarly, TWI in between 8-12 has the highest landslide density. In the case of the lithology, it can be seen that the FR for Upper Siwaliks is highest followed by Middle Siwalik and lowest for Sallyani Gad Formation (Table 2). The influence of a drainage system on the landslide susceptibility was also analyzed by identifying the drainage density which was found to be varying from 0-9 and has a positive influence on landslide density. Barren land cover can be seen as highly susceptible for the landslide with Riverbanks value 4.1 followed by Barren land and Grassland.

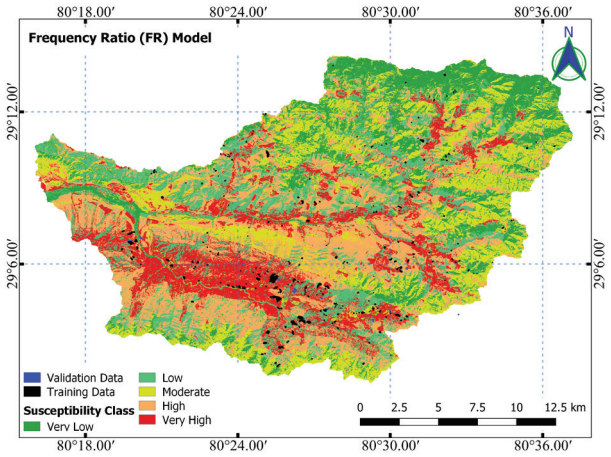

Fig. 4: Landslide susceptibility map derived from the frequency ratio (FR) model.

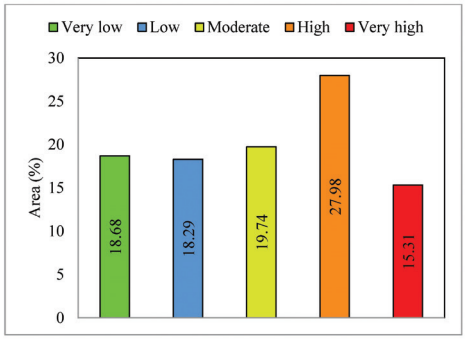

Fig. 5: Area covered by different susceptibility classes based on frequency ratio (FR) model.

Landslide susceptibility map using the logistic regression model

The logistic regression was carried out in R-Studio to estimate the coefficients for each independent variable in the intercept. The following Equation 7 is implemented and the raster calculator in ArcGIS 10.5 is then used to obtain the susceptibility map.

$$z = -2.738 + (Aspect \times 0.0019) + (\text{Drainage density} \times -0.0046) + (\text{Elevation} \times -0.002) + (\text{Distance from fault} \times -0.00001) + (\text{Lithology} \times -0.000001) + (\text{LULC} \times -0.00001) + (\text{NDVI} \times -0.0002) + (\text{Plane curvature} \times 0.066) + (\text{TWI} \times -0.004) + (\text{Slope} \times 0.075), \quad (7)$$

The analysis of the logistic regression coefficients (β-coefficients) depicts slope gradient, slope aspect, elevation, and plane curvature have prominent role in landslide susceptibility with positive β-coefficients. Similarly, drainage density, distance from fault, and NDVI lithology all have a negative impact on landslide formation because they all have a negative β-coefficient and are thus regarded less important in landslide formation.

The susceptibility range of the landslide obtained by LR model ranges between (0-1) and was categorized into five classes namely Very low, Low, Moderate, High and Very high based upon natural break technique. The final susceptibility map developed form this model is shown in Figure 6. From the analysis of logistic regression model also most of the area high susceptibility zone covering 25.55% of the study area followed by moderate susceptibility zone with 22.81 %. Very high susceptibility zone covers the least area i.e. 13.99 % and very low susceptibility region covers 20.94 % of the study area (Fig. 7).

Table 2: Spatial relationship between each landslide conditioning factor and landslide by frequency ratio model.

LCFs	Class	Landslide Area (m^2)	FR	PR
Elevation	250-542	1406.25	0.04	3.467
	542-773	502968.75	1.69	
	773-995	648906.25	1.63	
	995-1226	101093.75	0.54	
	1226-1475	19531.25	0.15	
	1475-1742	8593.75	0.08	
	1742-2044	10937.50	0.14	
	2044-2524	1875.00	0.04	
Slope Gradient	0-15	94687.50	0.44	2.624
	15-30	233437.50	0.70	
	30-45	395312.50	1.10	
	45-60	327500.00	1.22	
	60-76.5	244375.00	2.05	
Plane Curvature	Concave	676562.50	1.19	2.079
	Flat	80781.25	0.57	
	Convex	537968.75	0.92	
Slope Aspect	Flat	58593.75	0.38	1.480
	N	108906.25	0.89	
	NE	172500.00	1.54	
	E	203125.00	1.47	
	SE	249531.25	1.67	
	S	285937.50	1.66	
	SW	132812.50	0.89	
	W	56093.75	0.39	
	NW	27812.50	0.18	
TWI	-3-4	354218.75	1.19	1.000
	4-8	287187.50	0.85	
	8-12	653906.25	0.99	
Drainage Density	0-2	339218.75	0.55	2.570
	2-4	486250.00	1.41	
	4-6	377968.75	1.84	
	>6	91875.00	0.71	
Lithology	Bu	26875.00	0.71	4.054
	Basic Rocks	43437.50	0.20	
	SGF	5468.75	0.08	
	Granites	7500.00	0.21	
	Gn	21406.25	0.39	
	SGF	23906.25	0.36	
	SYF	17968.75	0.30	
	SAF	20625.00	0.38	
	Lower Siwalik	85781.25	0.39	
	Upper Siwalik	762968.75	3.51	
	Middle Siwalik	279375.00	1.09	
Distance from fault	0-200	226875.00	2.09	1.570
	200-400	165468.75	1.57	
	400-600	76093.75	0.74	
	600-800	168437.50	1.71	
	800-1000	108125.00	1.19	
	>1000	550312.50	0.70	

LCFs	Class	Landslide Area (m^2)	FR	PR
NDVI	<0.2	6562.50	0.21	5.683
	0.2-0.6	1051718.75	1.28	
	0.6-0.8	237031.25	0.54	
	>0.8	0.00	0.00	
LULC	Cultivation	143125.00	2.51	3.430
	Forest	223906.25	0.26	
	Barren	442031.25	4.98	
	Grassland	370468.75	1.31	
	River and Bank	115781.25	6.01	
SPI	0-150	1109843.75	0.98	0.570
	150-300	82812.50	1.15	
	300-450	30625.00	1.26	
	>450	72031.25	1.04	

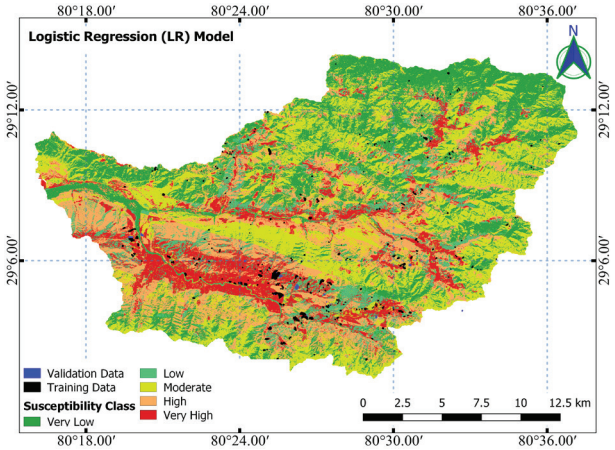

Fig. 6: Landslide susceptibility map derived from the logistic regression (LR) model.

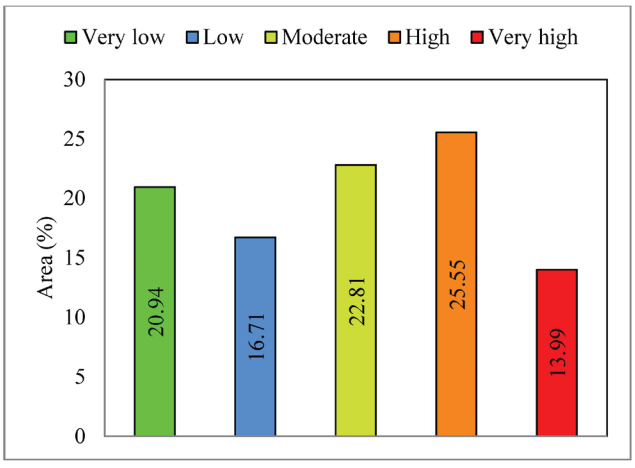

Fig. 7: Area covered by different susceptibility classes based on logistic regression (LR) model.

Validation of the susceptibility models

In this study, the performance of the FR and LR model has been evaluated using the success rate and prediction rate curves. The success rate curve was prepared by using the relationship between the percentage of landslide susceptibility map and the percentage of landslide pixels used for the training process (70%) whereas validation data (30%) were used to generate a prediction rate curve. The success rate and prediction rate curve for both models are presented in Figure 8. The area under the receiver operating characteristic curve (AUC) explains the degree of fit of the models in terms of success rate and prediction rate. The success rate shows how well the resulting landslide map is classified using the existing landslides while the prediction rate indicates the predictive power of the landslide map (Jaafari et al., 2014).

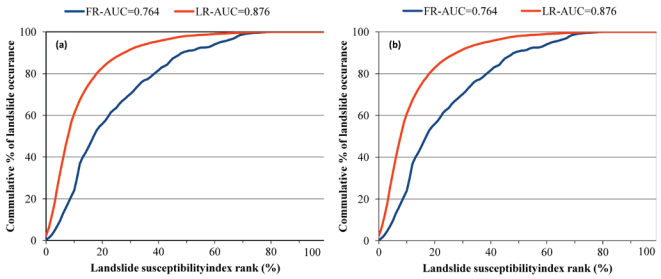

Fig. 8: Validation of the susceptibility models (a) Success rate of the landslide susceptibility maps. (b) Prediction rate of the landslide susceptibility maps.

The AUC was obtained using 100 subdivisions of all the cells in the study area's LSI values and the cumulative percentage of landslide occurrences in the classes. Both the training and validation data were used to calculate the AUC. From the AUC curve, it can be observed that the success rate is 87.6% for the LR model with a prediction rate of 87.3% indicating a good degree of fit. With a success rate of 76.4% and a prediction rate of 75.1%, the result obtained from the FR model is a fairly good performance but the LR model seems to be better for the study area.

DISCUSSION

Landslide inventory

Geomorphologic hazards in the Hindu Kush regions have been evolved due to weak geological environments, diversified rock types, high degree of rock weathering, varying topography,

the high gradient of rivers, seasonal precipitation, and changes in climatic conditions (Dhakal, 2015). The distribution of the number and size of the landslides in the study area is not homogenous and was found to be varying with geology and morphology as mentioned by (Pathak and Devkota, 2022). The extent of the present study area falls under the Mahabharat range and Sub-Himalaya Range. Dhital (2015) has differentiated the Sub- Himalaya of the portion between Mahakali–Seti Rivers into the Lower Siwaliks, Middle Siwaliks and Upper Siwaliks. This division of the Siwalik zone into three formations based on lithology and stratigraphy by various researchers (Devkota et al., 2012; Dhakal, 2015; Dhital, 2015) and also found variation in landslide dynamics along with these divisions (Bhandari and Dhakal, 2020).

The elevation ranges from 258 to 2,500 m within a very small area and has a higher slope gradient and profile. Along with the sedimentary rock, this caused slope instability, and various slope movements like rock fall, rock flow, rock slides, and complex types (Cruden and Varnes, 1996) were observed in the study area. The distribution of the small landslides in the study area is due to the fragile nature of the Siwalik region, whereas the occurrence of medium and large size sized landslides is due to the presence of active fault passes close to the main boundary thrust and runs through Budar, Alital, and Kalena. In the south of this active fault, Budar thrust delimits the Siwaliks from the Mahabharat Range. The higher density of the small and medium-sized landslides in this study area is a similar result to that of the previous study (Bhandari and Dhakal, 2020). The densities of the landslide were found higher in the vicinity of these faults and thrust. This shows that the landslide mobility in the study area is greatly affected by lithology along with terrain height and slope. Currently, there are two very large-sized landslides found to be active and the morphology shows the evolution of the landscape found to be greatly influenced by landslide events. As concluded by Fort et al. (2009), landslide events may influence landscape morphology and evolution for thousands of years.

Landslide susceptibility

Landslide susceptibility evaluation from both models gives little bit different results this is due to their capacity of prediction based upon the LCFs considered. In the case of the FR model highest weightage was of NDVI followed by lithology indicating the vital role of vegetation for landslide occurrence. Similarly, lithology also plays an important role because the types of rock and their weathering status differ in different lithology. Weathering processes affect rock types at different rates, making some more susceptible to weathering and therefore weaker (Dhakal, 2015). Also, unstable bedding sequences can lead to weaknesses within the geology, intensified by weathering processes, faulting, and tectonic uplift, fracturing, and folding, making them more susceptible to landslide (Duncan et al., 2003). Along the elevation up to a certain limit of about 1000 m, the landslide frequency was higher (Table 2) with a frequency ratio greater than one for 500 to 750 and 750 to 1000 classes. This can be due to most of the portion of Upper and Lower Siwaliks falling under this class and which is considered a landslide-prone area from past studies also (Bhandari and Dhakal, 2018, 2020; Devkota et al., 2012; TU-CDES, 2016). In the case of slope gradient, it is seen that landslides are higher in slopes >30°. The FR value is highest for slope class ≥ 60°, followed by the 45- 60° slope class. This is due to the reason that the shear stress in the soil or other unconsolidated material generally increases with an increase in the slope angle. Generally, gentle slopes are expected to have a low frequency of landslides because of the lower shear stresses that are related to low gradients (Regmi et al., 2014). From the value of frequency ratio, the slope aspect shows that the SE-facing slopes are most affected by landslides, followed by S-, NE, and E-facing slopes.

The distance between 0 and 200 m from the fault shows a higher correlation with the landslides. The relation between a landslide and its distance to a fault line shows that, when the distance from the fault line increases, the landslide occurrence probability decreases, and densities of the landslide are found higher in the vicinity of faults and thrust. The drainage density also has a great influence on landslide formation in the study area. The relation between TWI and landslide probabilities showed that the -3–5 classes have the highest FR value. In the case of land use, higher FR values were associated with the area around the river which has toe cutting effect upon the surrounding slope. Similarly, barren land is also found to be prone to landslides. From the analysis of logistic regression coefficients, it is seen that slope angle, curvature, NDVI, and lithology have a prominent role in the landslide susceptibility of the area, as they all have positive β values. Also, it is seen that SPI is not significant LCF for susceptibility analysis by using the LR model.

The area covered by the different susceptible zones in landslide susceptible maps from both methods is not exactly overlapped implying that if a factor class has lower and higher values in both models, the susceptibility will also be lower and higher respectively. In case of FR model, the spatial relationship between the causative factors and landslide is determined by FR values where as in case of LR model it is determined by β values. Therefore validation was conducted to know the accuracy of the model used. As in landslide susceptibility assessment validation is very important and helps to identify the potential area of landslides and it is one of the preliminary steps for hazard and risk assessment (Jaafari et al., 2014). The AUC method used in this study is most widely used and used by several researchers (Devkota et al., 2012; Ghimire, 2011; Nepal et al., 2019; Regmi et al., 2014). In this study, the success rate is 87.6% for the LR model with a prediction rate of 87.3% indicating a good degree of fit. With a success rate of 76.4% and a prediction rate of 75.1%, the result obtained from the FR model was fairly good. Thus, the logistic model exhibited better similar performance, and can be regarded suitable for similar areas.

CONCLUSIONS

By considering the serious threat of landslides to the life, property, and environment this study is carried out to predict the susceptibility of landslide-prone areas. The total area covered by the landslides in the study area is 0.47%. For the prediction of landslide susceptible area landslide susceptibility map, based on frequency ratio (FR) and logistic regression (LR) model is implemented and susceptibility of the area divided into five groups. By using the FR model in the study area largest portion falls under the high susceptibility zone which covers 27.98 % of the total area. Similarly 19.74%, 18.29%,

18.68%, and 15.31% area is covered by moderate, low, very low and very high susceptibility zone, respectively. Similarly, from the analysis of the logistic regression, 25.55 % of the area found to be high susceptible to landslide followed by moderate susceptibility zone with 22.81 %. Very high susceptibility zone covers the least area i.e. 13.99 % and very low susceptibility region covers 20.94 % of the study area. Coefficients of the logistic regression (β-coefficients) depict slope gradient, slope aspect, elevation, and plane curvature have prominent role in landslide susceptibility and with negative β coefficient drainage density, distance from fault, and NDVI can be considered less important in landslide occurrence.

The validity of the models was confirmed by using the relationship between the percentage of landslide susceptibility map and the percentage of landslide pixels used for the training process (70%) whereas validation data (30%) were used to generate a prediction rate curve. The success rate is 87.6% for the LR model with a prediction rate of 87.3% indicating a good degree of fit. With a success rate of 76.4% and a prediction rate of 75.1%, the result obtained from the FR model is a fairly good performance but the LR model seems to be better for the study area.

ACKNOWLEDGMENTS

The authors are thankfull to the Central Department of Environmental Science, different reviewers, and the Department of Environment, Ministry of Forests and Environment, Nepal for granting this research.

REFERENCES

Bhandari, B. P. and Dhakal, S., 2018, Lithological Control on Landslide in the Babai Khola Watershed, Siwaliks Zone of Nepal. American Journal of Earth Sciences, v. 5, pp. 54–64.

Bhandari, B. P. and Dhakal, S., 2020, Spatio-temporal dynamics of landslides in the sedimentary terrain: a case of Siwalik zone of Babai watershed, Nepal. SN Applied Sciences, v. 2. https://doi.org/10.1007/s42452-020-2628-0.

Bhandari, D., Joshi, R., Regmi, R. R., and Awasthi, N., 2021, Assessment of Soil Erosion and Its Impact on Agricultural Productivity by Using the RMMF Model and Local Perception: A Case Study of Rangun Watershed of Mid-Hills, Nepal. Applied and Environmental Soil Science, 2021. https://doi.org/10.1155/2021/5747138.

Brabb, E. E., 1985, Innovative approaches to landslide hazard and risk mapping. International Landslide Symposium Proceedings, Toronto, Canada, v. 1, pp. 17–22.

Budimir, M. E. A., Atkinson, P. M., and Lewis, H. G., 2015, A systematic review of landslide probability mapping using logistic regression. Landslides, v. 12, pp. 419–436.

CBS, 2011, National Population and Housing Census. Central Bureau of Statistics (CBS), Nepal.

CDES-TU and PCTMCDB, 2017, Landslide Atlas of Chure Region 2017 with characterization and Mitigation Design, Part II. President Chure-Tarai Madhesh Conservation Development Board, Government of Nepal, Kathmandu and Central Department of Environmental Science, Tribhuvan University, Kirtipur, Kathmandu.

Cruden, D. M. and Varnes, D. J., 1996, Landslide Types and Processes. In Landslides: Investigation and Mitigation. National Academy Press. (Issue Bell 1992), pp. 36–75.

D'Odorico, P., Gonsamo, A., Damm, A., and Schaepman, M. E., 2013, Experimental evaluation of sentinel-2 spectral response functions for NDVI time-series continuity. IEEE Transactions on Geoscience and Remote Sensing, v. 51, pp. 1336–1348.

Dahal, R. K., 2012, Rainfall-induced landslides in Nepal. International Journal of Erosion Control Engineering, v. 5, pp. 1–8.

Dahal, R. K. and Hasegawa, S., 2008, Representative rainfall thresholds for landslides in the Nepal Himalaya. Geomorphology, v. 100(3-4), pp. 429–443.

Devkota, K. C., Regmi, A. D., Pourghasemi, H. R., Yoshida, K., Pradhan, B., Ryu, I. C., Dhital, M. R., and Althuwaynee, O. F., 2012, Landslide susceptibility mapping using certainty factor, index of entropy and logistic regression models in GIS and their comparison at Mugling-Narayanghat road section in Nepal Himalaya. Natural Hazards, v. 65, pp.135–165.

Dhakal, S., 2013, Geological hazards in Nepal and triggering effect of climate change. Bull. Nepal Geol. Soc., v. 30, pp. 75–80.

Dhakal, S., 2014a, Geological Divisions and Associated Hazards in Nepal. In Contemporary Environmental Issues and Methods in Nepal, pp. 100–109.

Dhakal, S., 2014b, Disaster in Nepal, In: Disaster Risk Management: Concept, Policy and Practices in Nepal, Central Department of Environmental Science (CDES), Tribhuvan University Kirtipur.

Dhakal, S., 2015, Evolution of geomorphologic hazards in Hindu Kush Himalaya. In Mountain hazards and disaster risk reduction. Springer, pp. 53–72.

Dhital, M. R., Upreti, B. N., Dangol, V., Bhandari, A. N., and Bhattarai, T. N., 1991, Engineering geological methods applied in mountain road survey-an example from Baitadi-Darchula road project (Nepal). Jour. Nepal Geol. Soc., v. 7, pp.49–67.

Dhital, M. R., 2000, An overview of landslide hazard mapping and rating systems in Nepal. Jour. Nepal Geol. Soc., v. 22, pp. 533–538.

Dhital, M. R., 2015, Geology of the Nepal Himalaya. In Springer International Publishing Switzerland, pp. 81–91.

DMG, 2020, Geological Map of Sudurpaschim Province, Scale: 1:350,000, Department of Mines and Geology (DMG), Government of Nepal, Kathmandu.

Duncan, C., Masek, J., and Fielding, E., 2003, How steep are the Himalaya? Characteristics and implications of along-strike topographic variations. Geology, v. 31, pp. 75–78.

Fort, M., Cossart, É., Deline, P., Dzikowski, M., Nicoud, G., Ravanel, L., Schoeneich, P., and Wassmer, P., 2009, Geomorphic impacts of large and rapid mass movements: a review. v. 15, pp. 23–34.

Galli, M., Ardizzone, F., Cardinali, M., Guzzetti, F., and Reichenbach, P., 2008, Comparing landslide inventory maps. Geomorphology, v. 94(3-4), pp. 268–289.

Ghimire, M., 2011, Landslide occurrence and its relation with terrain factors in the Siwalik Hills, Nepal: Case study of susceptibility assessment in three basins. Natural Hazards, v. 56, pp. 299–320.

Guzzetti, F., Reichenbach, P., Cardinali, M., Galli, M., and Ardizzone, F. 2005, Probabilistic landslide hazard assessment at the basin scale. Geomorphology, v. 72, pp. 272–299.

Jaafari, A., Najafi, A., Pourghasemi, H. R., Rezaeian, J., and Sattarian, A., 2014, GIS-based frequency ratio and index of entropy models for landslide susceptibility assessment in the Caspian forest,

northern Iran. International Journal of Environmental Science and Technology, v. 11, pp. 909–926.

Lee, S., 2007, Landslide susceptibility mapping using an artificial neural network in the Gangneung area, Korea. International Journal of Remote Sensing, v. 28, pp. 4763–4783.

Lee, S. and Talib, J. A., 2005, Probabilistic landslide susceptibility and factor effect analysis. Environmental Geology, v. 47, pp. 982–990.

Lee, Saro, and Pradhan, B., 2007, Landslide hazard mapping at Selangor, Malaysia using frequency ratio and logistic regression models. Landslides, v. 4, pp. 33–41.

Li, Z., Zhu, C., and Gold, C., 2004, Digital terrain modeling: principles and methodology. CRC press.

MoHA, 2019, Nepal Disaster Report 2019. In Ministry of Home Affairs (MoHA), Government of Nepal.

Moore, I. D. and Grayson, R. B., 1991, Terrain-based catchment partitioning and runoff prediction using vector elevation data. Water Resources Research, v. 27, pp. 1177–1191.

Nepal, N., Chen, J., Chen, H., Wang, X., and Pangali Sharma, T. P., 2019, Assessment of landslide susceptibility along the Araniko Highway in Poiqu/Bhote Koshi/Sun Koshi Watershed, Nepal Himalaya. Progress in Disaster Science, v. 3. https://doi.org/10.1016/j.pdisas.2019.100037.

Pantha, B. R., Yatabe, R., and Bhandary, P., 2008, GIS-based landslide susceptibility zonation for roadside slope repair and maintenance in the Himalayan region, v. 31(4), pp. 384–391.

Pardeshi, S. D., Autade, S. E., and Pardeshi, S. S., 2013, Landslide hazard assessment: Recent trends and techniques. SpringerPlus, v. 2, pp. 1–11.

Pathak, L. and Devkota, K. C., 2022, Distribution and Dynamic Behaviors of Landslide in Rangun Khola Watershed of the Western Nepal, Journal of Environment Sciences., v. 8, pp. 68–79.

Pathak, L., Pant, R. R., Khadka, U. R., Nepal, J., Poudel, S., Pathak, G., and Thapa, L. B., 2020, Spatial analysis of water stress and application of water poverty index in the Mahakali River Basin, Sudurpaschim Province, Nepal. Nepalese Journal of Zoology, v. 4(2), pp. 85–94.

Paudyal, K. R., Devkota, K. C., Parajuli, B. P., Shakya, P., and Baskota, P., 2021, Landslide Susceptibility Assessment using Open-Source Data in the Far Western Nepal Himalaya: Case Studies from Selected Local Level Units. Journal of Institute of Science and Technology, v. 26, pp. 31–42.

Petley, D. N., Hearn, G. J., Hart, A., Rosser, N. J., Dunning, S. A., Oven, K., and Mitchell, W. A., 2007, Trends in landslide occurrence in Nepal. Natural Hazards, v. 43, pp. 23–44.

Pham, B. T., Bui, D. T., Prakash, I., and Dholakia, M. B., 2015, Landslide Susceptibility Assessment at a Part of Uttarakhand Himalaya, India using GIS – based Statistical Approach of Frequency Ratio Method. International Journal of Engineering Research and Technology (IJERT), v.4. https://doi.org/10.17577/IJERTV4IS110285.

Pourghasemi, H. R., Teimoori Yansari, Z., Panagos, P., and Pradhan, B., 2018, Analysis and evaluation of landslide susceptibility: a review on articles published during 2005–2016 (periods of 2005–2012 and 2013–2016). Arabian Journal of Geosciences, v. 11. https://doi.org/10.1007/s12517-018-3531-5.

Pradhan, B. and Lee, S., 2010, Landslide susceptibility assessment and factor effect analysis: backpropagation artificial neural networks and their comparison with frequency ratio and bivariate logistic regression modelling. Environmental Modelling and Software, v. 25, pp. 747–759.

Pradhan, B., Oh, H. J., and Buchroithner, M., 2010, Weights-of-evidence model applied to landslide susceptibility mapping in a tropical hilly area. Geomatics, Natural Hazards and Risk, v. 1, pp. 199–223.

Regmi, A. D., Devkota, K. C., Yoshida, K., Pradhan, B., Pourghasemi, H. R., Kumamoto, T., and Akgun, A., 2014, Application of frequency ratio, statistical index, and weights-of-evidence models and their comparison in landslide susceptibility mapping in Central Nepal Himalaya. Arabian Journal of Geosciences, v. 7, pp. 725–742.

Saha, A. K., Gupta, R. P., Sarkar, I., Arora, M. K., and Csaplovics, E., 2005, An approach for GIS-based statistical landslide susceptibility zonation-with a case study in the Himalayas. Landslides, v. 2, pp. 61–69.

Schweigl, J. and Hervas, J., 2009, Landslide mapping in Austria. In JRC Scientific and Technical Reports EUR 23785 EN.

Sezer, E. A., Pradhan, B., and Gokceoglu, C., 2011, Manifestation of an adaptive neuro-fuzzy model on landslide susceptibility mapping: Klang valley, Malaysia. Expert Systems with Applications, v. 38, pp. 8208–8219.

Shao, X., Ma, S., Xu, C., Shen, L., and Lu, Y., 2020, Inventory, distribution and geometric characteristics of landslides in Baoshan City, Yunnan Province, China. Sustainability (Switzerland), v.12. https://doi.org/10.3390/su12062433.

Thapa, P. B., 2015, Occurrence of landslides in Nepal and their mitigation options. Journal of Nepal Geological Society, v. 49, pp. 17–28.

TU-CDES, 2016, Landslide Inventory Characterization and Engineering Design for Mitigation Works of Chure Area in Ten Districts.

Yilmaz, C., Topal, T., and Lu, M., 2011, GIS-based landslide susceptibility mapping using bivariate statistical analysis in Devrek (Zonguldak-Turkey), pp. 2161–2178.